

Aerodynamic requirements assessment of civil aircraft based on airworthiness performance

Ruiqi Wang[1], Yan Liu[1], Mingxuan Zhang[1]

[1]Northwestern Polytechnical University

Abstract

Flight performance represents the comprehensive capability of an aircraft to accomplish a predefined mission and constitutes a primary objective in aircraft design. For civil aircraft, inferring aerodynamic requirements from flight performance metrics and airworthiness standards at the conceptual design stage can not only effectively mitigate the extensive and time-consuming iterative optimization processes inherent in traditional design methodologies, but also significantly shorten the initial aerodynamic design phase by improving both design efficiency and directional accuracy. In this paper, aerodynamic requirement constraints for civil aircraft are derived from performance indicators and airworthiness regulations across key flight phases, including takeoff, climb, cruise and landing, thereby providing quantitative aerodynamic references for the preliminary conceptual design Stage phase.

Keywords: Aerodynamic demand inversion; Flight performance; Airworthiness standard

1. General Introduction

For civil aircraft, flight performance not only directly affects operational economics and market competitiveness, but also constitutes a set of core constraints that must be satisfied during airworthiness certification. Takeoff and landing field lengths, which are representative airworthiness performance metrics, directly determine airport compatibility and operational flexibility[1]. Excessive field length requirements will significantly restrict the range of operable airports, thereby weakening the market adaptability of a civil aircraft. Meanwhile, the cruise phase, which accounts for the longest duration and the largest proportion of fuel consumption in a civil aircraft mission profile, plays a decisive role in overall economic performance[2]. By improving the cruise factor during the cruise phase, aerodynamic efficiency can be enhanced, thereby effectively reducing fuel consumption per unit range and increasing flight range, which significantly improves operational efficiency[3].

Therefore, establishing a quantitative mapping between flight performance requirements and key aerodynamic parameters at the early design stage, with airworthiness and mission performance metrics serving as constraints and design objectives, has become a critical issue for improving the effectiveness and efficiency of aerodynamic design. However, existing studies predominantly focus on the forward evaluation of flight performance under the assumption of known aerodynamic models[4]-[8], whereas publicly available research on the inverse derivation of aerodynamic requirements based on prescribed performance metrics remains relatively limited. To address this issue, this paper takes the performance requirements of key flight phases—including takeoff, climb, cruise, and landing—as inputs to inversely derive the corresponding aerodynamic requirements for each phase. This approach effectively avoids the frequent and time-consuming iterative optimization processes inherent in traditional design workflows, thereby significantly shortening the development cycle of the preliminary aerodynamic design stage and improving both design efficiency and directional accuracy.

2. Research Methods

For a civil aircraft, a complete mission profile includes the stages of taxi, takeoff, initial climb, climb

to cruise, cruise, descent, approach, landing, and taxi-out. Among these, the takeoff, climb, cruise, and landing phases are significantly influenced by aerodynamic and thrust characteristics. This paper focuses on the analysis of these four key phases. The calculation procedure for the aerodynamic requirements of each flight phase is shown in Figure 1 below.

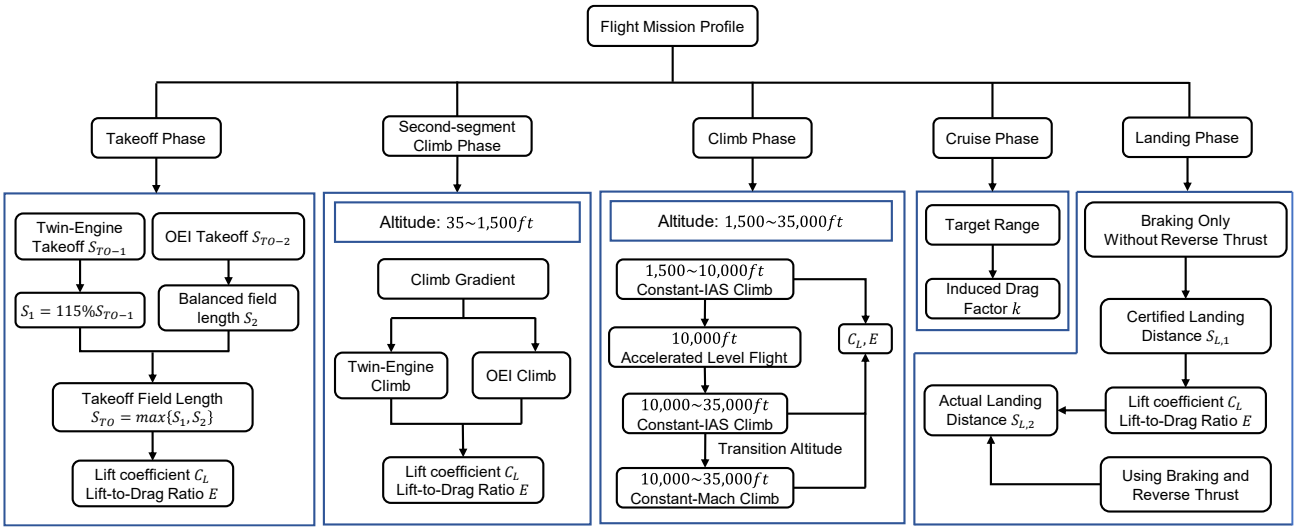


Figure 1 - Aerodynamic Requirements for Different Flight Phases

2.1 Takeoff Phase

The takeoff field length is defined as the greater of the following two distances:

(1) the horizontal distance from the start of the takeoff to the point where the aircraft reaches a height of 10.7 m above the takeoff surface, assuming that the critical engine fails on the ground at the engine failure speed V_{EF} and remains inoperative for the remainder of the takeoff;

(2) 115% of the horizontal distance from the start of the takeoff to the point where the aircraft reaches 10.7 m above the takeoff surface under conditions of all engines operating.

In the single-engine-inoperative (OEI) condition, the balanced field length is used as the distance in (1) for calculation purposes. During the takeoff phase, the required lift coefficient corresponding to a given takeoff field length is determined through an iterative procedure based on lift coefficient adjustments.

To prevent the derived aerodynamic requirements from being overly stringent and causing a waste of aerodynamic performance, this paper starts the iteration from a relatively small maximum lift coefficient and gradually increases it until the aerodynamic requirements necessary to meet the takeoff field length are obtained.

2.2 Second-segment climb Phase

The second-segment climb stage begins at an altitude of 35 ft following the completion of takeoff stage. After the aircraft reaches a height of 35 ft above the takeoff surface, it must continue the takeoff at a speed as close as practicable to, but not less than, V_2 until it reaches a height of 400 ft above the takeoff surface.

According to CCAR-25.111, during the flight segment between 35 ft and 400 ft altitude, with the landing gear retracted, the remaining engine(s) operating at takeoff thrust, the flaps maintained at the takeoff flap setting, and the airspeed held constant at V_2, the required climb gradient shall be no less than 0.024 for one-engine-inoperative conditions and no less than 0.027 for twin-engine-operating conditions.

2.3 Climb Phase

The en-route climb phase begins from an altitude of 1,500 ft, immediately following the completion of takeoff.

The standard climb trajectory shown in the following figure represents the mission profile of the climb phase.

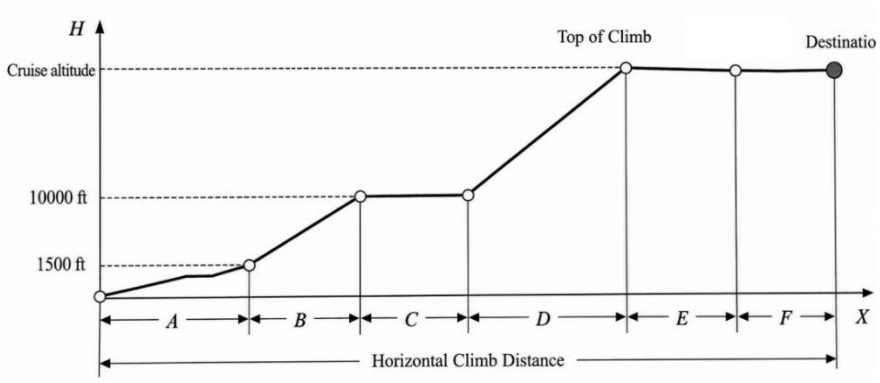


Figure 2 - Climb trajectory

Segment A&B: During this phase, the aircraft first performs an accelerating climb to an indicated airspeed of 250 kn , and then continues climbing at a constant indicated airspeed with a rate of climb of 2500 ft/min until reaching 10,000 ft.

Segment C: The aircraft accelerates in level flight at an altitude of 10,000 ft until reaching an indicated airspeed of 300 kn.

Segment D: During this phase, the aircraft first climbs at a constant indicated airspeed of 300 kn until the airspeed reaches Mach 0.785, corresponding to the transition altitude of 26,500 ft, and then continues climbing at a constant Mach number of 0.785.

2.4 Cruise Phase

In actual flight operations, considering air traffic control constraints, the aircraft maintains constant-altitude flight during the cruise phase, performs a cruise climb after a certain period, and then continues cruising at the new altitude. Therefore, the optimal aerodynamic parameters for the cruise phase should be evaluated based on the aircraft's performance under constant-altitude conditions. The initial cruise lift coefficient $C_{L,0}$ is assumed to be equal to the lift coefficient at the end of the climb segment, $C_{L,climb-end}$.

Since the aspect ratio has little influence on the zero-lift drag coefficient and mainly affects the induced drag factor k, a relatively large initial value of k and a target range R_0 are first specified. Using a step size of Δk, the constant-altitude and constant-speed range R corresponding to the lift coefficient under the current k value is calculated while gradually reducing k.

2.5 Landing Phase

The landing phase is divided into the airborne segment, the transition segment and the rollout segment. When determining the aerodynamic requirements for the landing phase, the certified landing field length should be taken into account. During this process, reverse thrust is not used, and deceleration is achieved solely through braking. The lift coefficient is iteratively adjusted according to the specified landing field length requirement until the certified landing distance meets the field length criterion.

Reverse thrust is used only during the actual landing phase. Since the thrust reverser mainly takes effect during the high-speed rollout phase, while the aircraft braking system mainly works during the low-speed phase, the effective time from touchdown to reverse-thrust operation is assumed to be 15 s. After that, the braking force becomes dominant. Therefore, the deceleration phase needs to be calculated in segments. The engine reverse thrust T_{rev} is taken as 40% of the takeoff thrust, while the engine idle thrust T_s corresponds to the thrust required for the aircraft to taxi on the ground at a speed of 20 knots.

3. Research Achievement

According to the above research methodology, the aerodynamic requirements corresponding to the flight performance indices for each flight phase are analyzed in detail. By combining the airworthiness regulations with the mission profile and flight performance constraints of the aircraft, the required

aerodynamic characteristics under different flight conditions are obtained through numerical simulation and iterative calculations.

The resulting analysis provides a systematic aerodynamic requirement reference for the preliminary aerodynamic design and modification of large-aspect-ratio civil aircraft. The obtained analysis results are summarized as follows.

3.1 Takeoff Phase

Considering a civil aircraft with a takeoff weight of 82,000 kg and a takeoff thrust of 150 kN per engine. The takeoff conditions correspond to standard sea-level atmosphere.

Given different takeoff field length requirements, the variations in aerodynamic requirements are shown in the figure below.

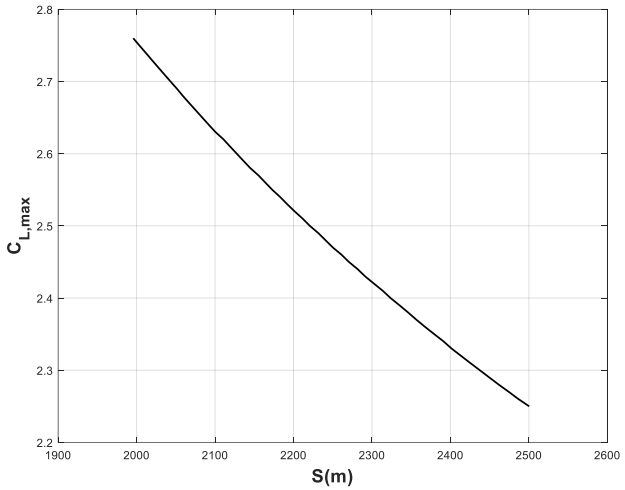


Figure 3 – Maximum Lift Coefficient

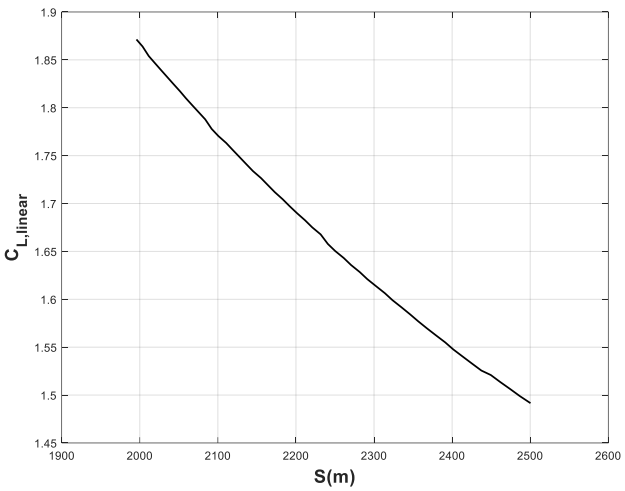


Figure 4 - Linear-Region Lift Coefficient

Based on the aerodynamic requirement analysis, it can be seen that the shorter the takeoff field length, the higher the requirements for the maximum lift coefficient and the linear-region lift coefficient in the takeoff configuration. This is because increasing the maximum lift coefficient reduces the stall speed V_S of the aircraft, which in turn reduces the corresponding rotation speed $1.1V_S$, thereby shortening the takeoff ground roll and reducing the required takeoff field length.

The aerodynamic requirement for the lift-to-drag ratio during the takeoff phase is shown in Figure 5. Once the linear-region lift coefficient exceeds the lift coefficient corresponding to the maximum lift-to-drag ratio, further increases in the linear-region lift coefficient will result in a continuous decrease of the lift-to-drag ratio.

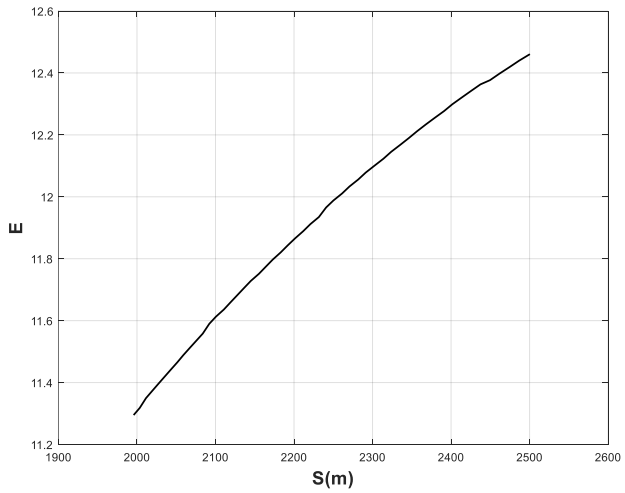


Figure 5 - Lift-to-Drag Ratio

Taking a takeoff field length of 2,400 m as an example, the simulation results for the takeoff phase under the corresponding aerodynamic requirements are shown in the figure below.

In the given aerodynamic conditions, the numerical simulation results for the ground roll, transition, and airborne phases during twin-engine takeoff are shown in Figure 6 -Figure 8. During the ground roll phase, the aircraft accelerates from zero speed to the nose-wheel lift-off speed. During this process, the lift L increases continuously while the ground reaction force R decreases. In the transition phase, the aircraft continues to accelerate and pitches up from the nose-wheel lift-off speed. During this phase, the velocity V, angle of attack α, and lift L increase continuously until the ground reaction force reduces to $R = 0$,marking the end of the transition phase and lift-off. In the airborne phase, the aircraft accelerates and climbs under the action of the remaining thrust until the flight height reaches 35 ft.

The solution diagram of the balanced field length is shown in Figure 9.

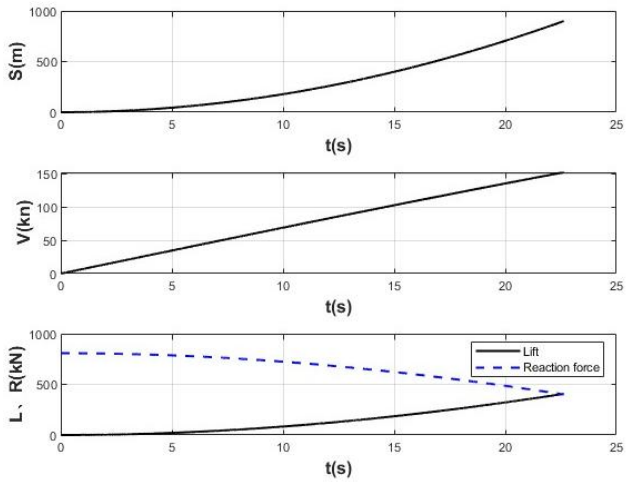


Figure 6 – Ground roll phase

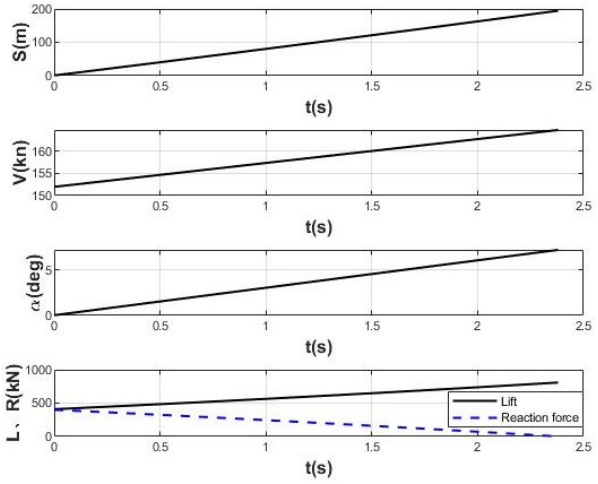


Figure 7 – Transition phase

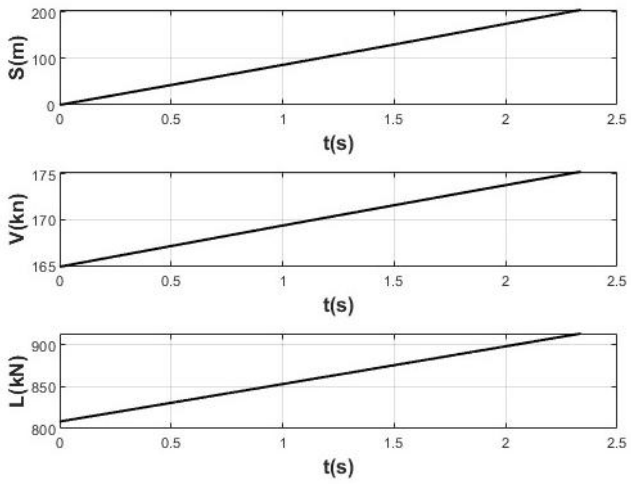


Figure 8 - Airborne Phase

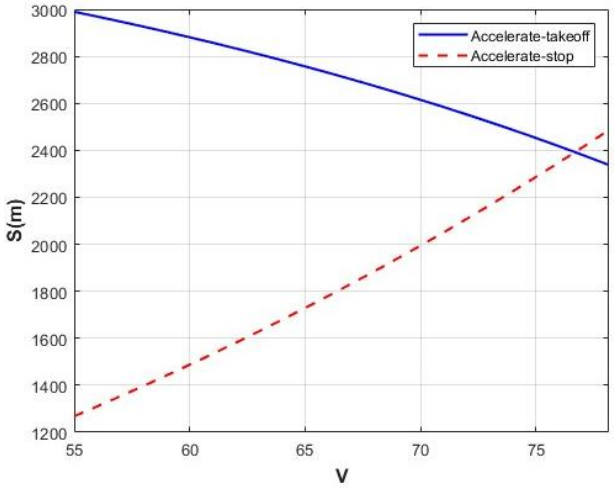


Figure 9 - Balanced Field Length

3.2 Second-segment climb Phase

Under the prescribed climb gradient requirement of 2.7% (twin-engine) and 2.4% (one-engine-inoperative, OEI), the aircraft altitude and airspeed, as well as the required lift-to-drag ratio and lift coefficient during the twin-engine climb are shown in Figure 10, Figure 11 and Figure 12respectively.

During this phase, the variation in aircraft speed is relatively small, mainly due to the low flight speed and the consequently large induced drag. Since the climb gradient is specified and the aircraft speed changes only slightly, the altitude increases approximately linearly.

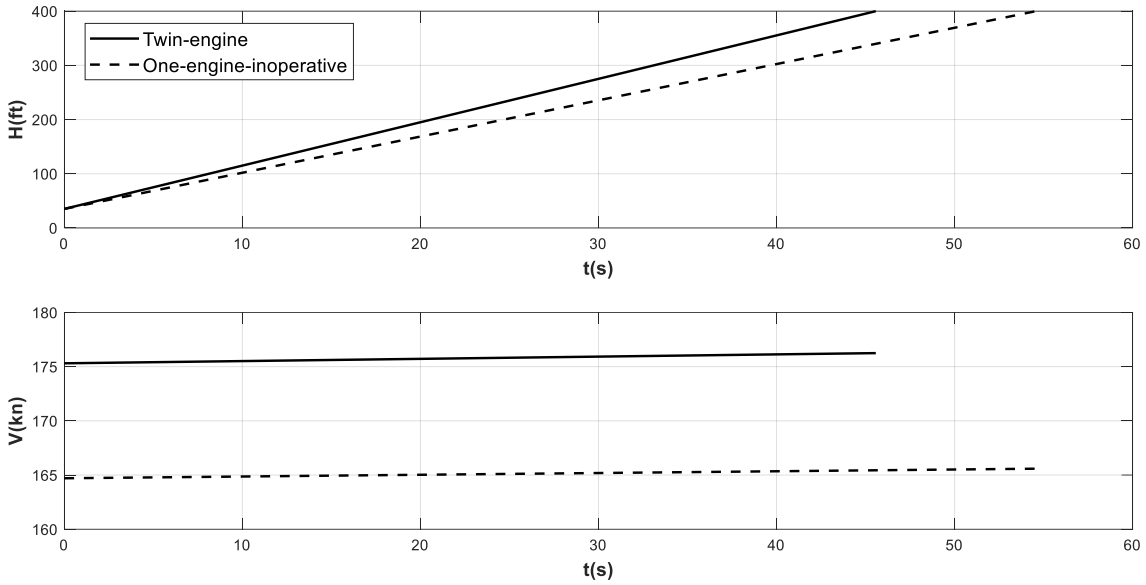


Figure 10 - Simulation Parameters for the OEI Second-Segment Climb

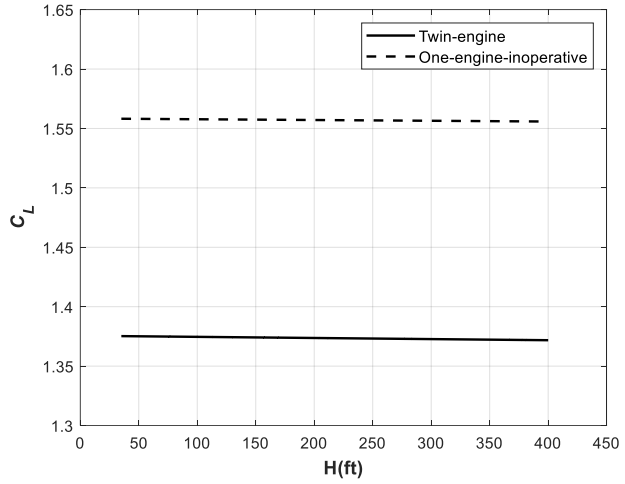


Figure 11 - Lift Coefficient

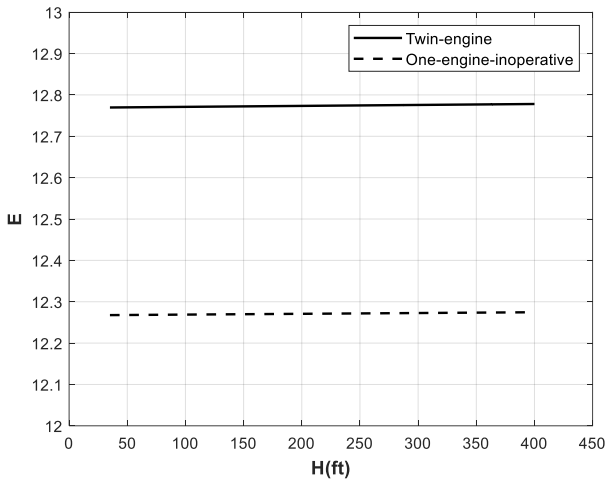


Figure 12 - Lift-to-Drag Ratio

Conclusion: To satisfy the 2.7% climb gradient requirement during the twin-engine climb, the aircraft lift-to-drag ratio should be greater than 12.77, and the lift coefficient should be greater than 1.37.

To satisfy the 2.4% climb gradient requirement during the twin-engine climb, the aircraft lift-to-drag ratio should be greater than 12.27, and the lift coefficient should be greater than 1.56.

3.3 Climb Phase

The climb phase is simulated in segments according to the flight climb trajectory.

3.3.1 $\mathbf{400{\sim}10000}\boldsymbol{ft}$ climb

During this phase, the aircraft first performs an accelerating climb to an indicated airspeed of 250 kn, and then continues climbing at a constant indicated airspeed with a rate of climb of 2500 ft/min until reaching 10,000 ft.

The variations in flight altitude, indicated airspeed, rate of climb, and thrust during this phase are shown in Figure 13.

It can be observed that during the accelerating climb segment, the climb angle decreases rapidly as the airspeed increases while the rate of climb remains constant, resulting in a relatively high required thrust. During the constant indicated airspeed climb phase, the true airspeed increases gradually with altitude, and the climb angle decreases slowly, leading to a lower required thrust.

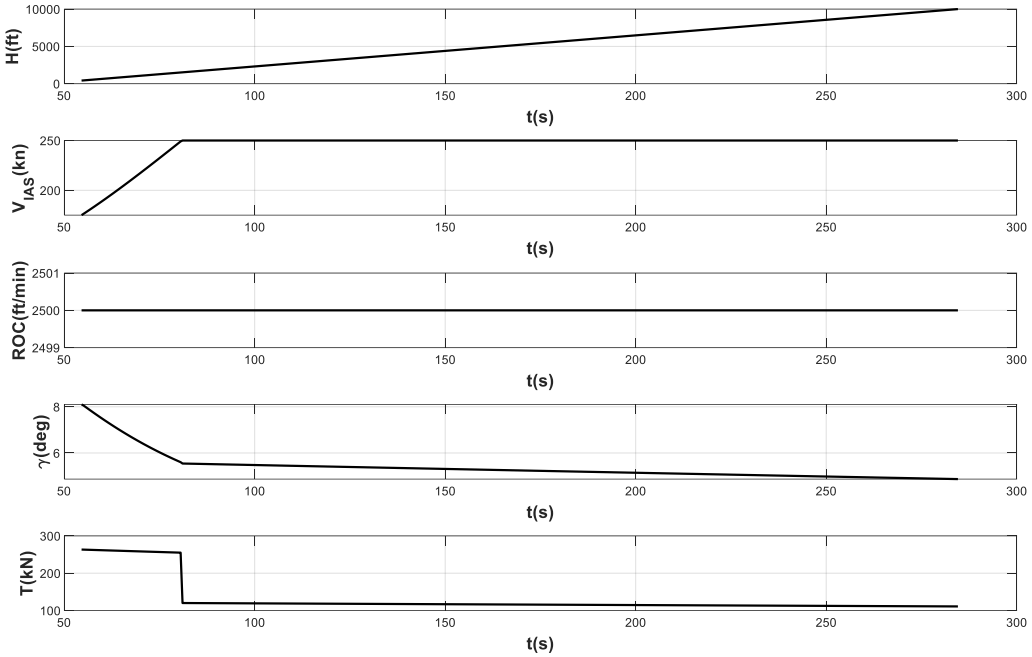


Figure 13 - Simulation results

The variations in the aircraft aerodynamic requirements during this phase are shown in Figure 14 and Figure 15. During the accelerating climb segment, although the reduction in climb angle causes the aircraft lift to increase slightly, the rapid increase in airspeed leads to a significant decrease in the lift coefficient. Since the drag first decreases with increasing speed until reaching the minimum-drag speed and then increases again, the lift-to-drag ratio exhibits a trend of first increasing and then decreasing. The maximum lift-to-drag ratio shown in Figure 15 corresponds to the aircraft maximum lift-to-drag ratio.

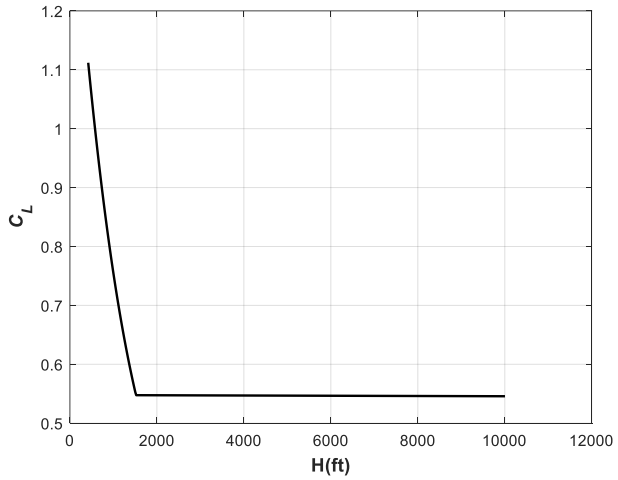


Figure 14 - Lift Coefficient Requirement during the 400–10,000 ft Climb Segment

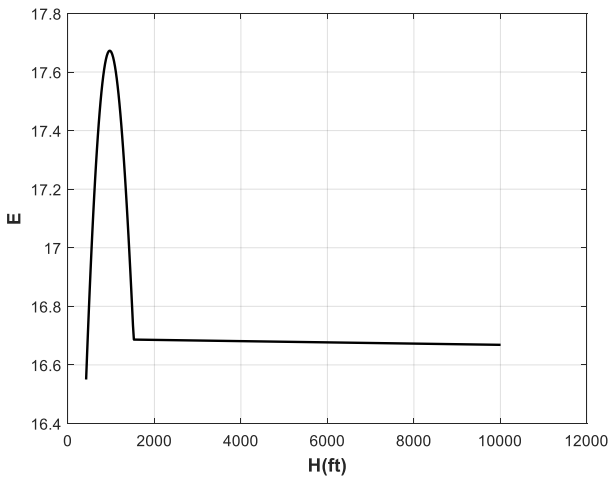


Figure 15 - Lift-to-drag ratio Requirement during the 400–10,000 ft Climb Segment

It can be seen that the maximum required lift-to-drag ratio of the aircraft is approximately 17.67, corresponding to a lift coefficient of approximately 0.77.

3.3.2 Accelerated level flight Stage

During this phase, the aircraft accelerates in level flight at an altitude of 10,000 ft until reaching an indicated airspeed of 300 kn. The acceleration process is shown in Figure 16. During this phase, only the airspeed is increased, and no special aerodynamic requirements are imposed.

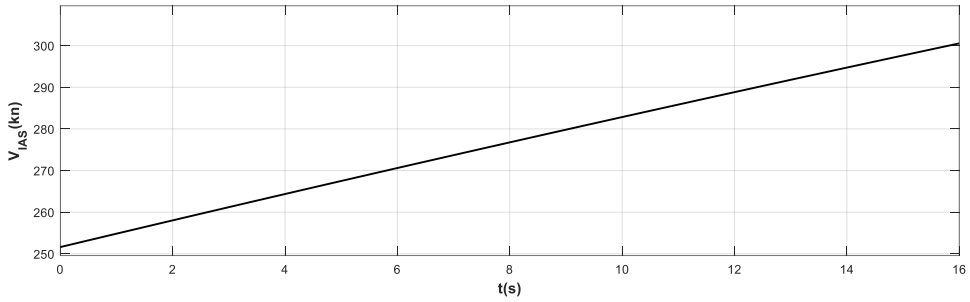


Figure 16 - Velocity variation

3.3.3 $\mathbf{10000{\sim}35000}\boldsymbol{ft}$ climb

During this climb phase, the aircraft first performs an accelerating climb at a constant indicated airspeed of 300 kn until reaching Mach 0.785, and then continues climbing at a constant Mach number.

The variations in flight altitude, Mach number, rate of climb, and thrust during this phase are shown in Figure 17. In this phase, the initial rate of climb is 2000 ft/min, while at the top of climb, the rate of climb decreases to 300 ft/min.

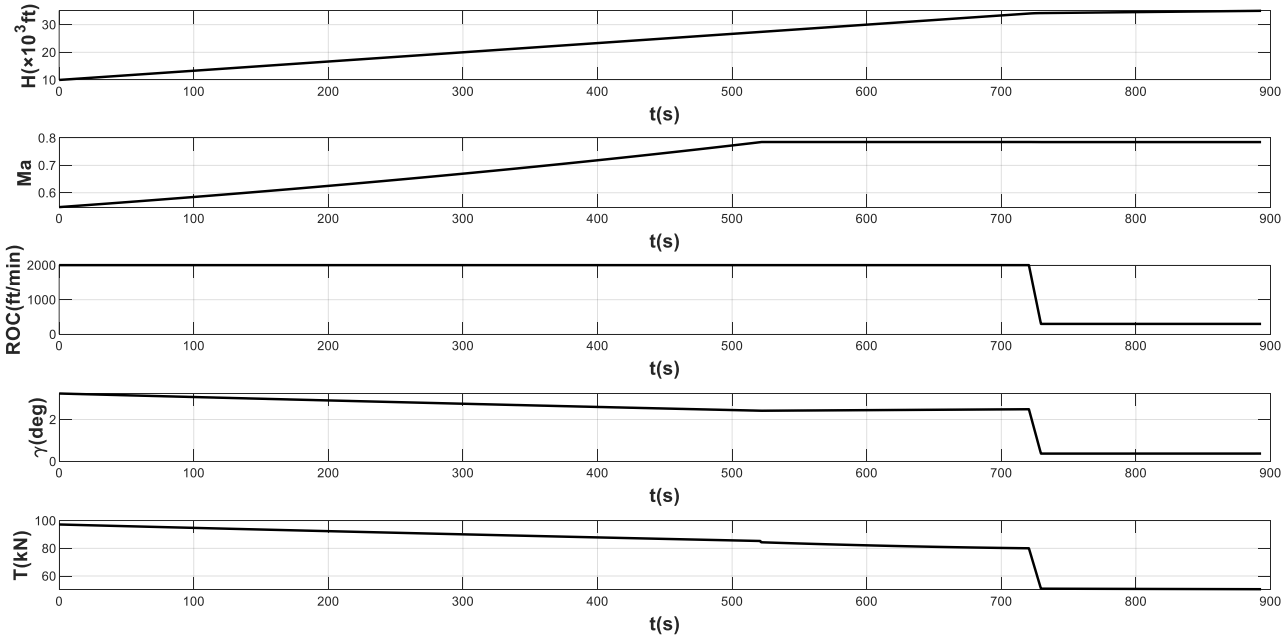


Figure 17 - Simulation Results for the 10,000–35,000 ft Climb Segment

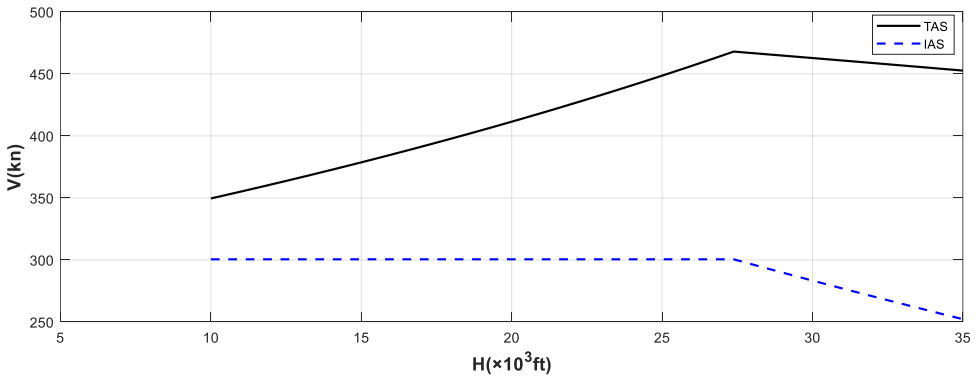


Figure 18 - Comparison between IAS and TAS

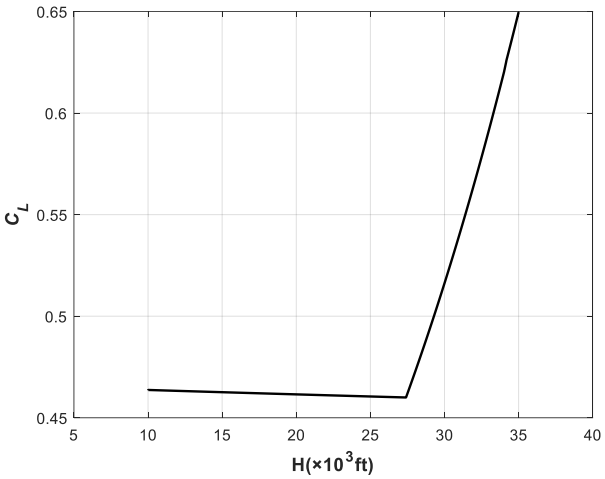


Figure 19 - Variation of Lift Coefficient

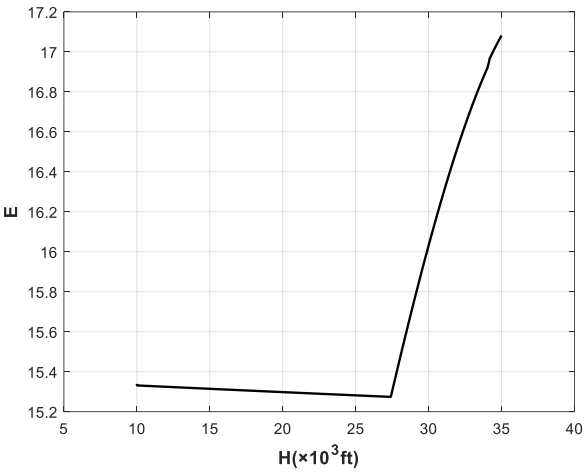


Figure 20 - Variation of Lift-to-Drag Ratio

At the top of the climb segment, the aircraft lift coefficient is 0.65, and the lift-to-drag ratio is 17.07.

Throughout the entire climb phase, namely from 35 ft above ground level to 35,000 ft, the aircraft fuel consumption is 1817.8 kg.

3.4 Cruise Phase

Considering the cruise phase, the aircraft consumes 80% of the total fuel, corresponding to 15,648 kg. The initial cruise weight is assumed to be equal to the aircraft weight at the top of climb, namely 82,000−115.8−1817.8=80,066 kg. Therefore, at the end of cruise, the aircraft weight decreases to 64,418 kg.

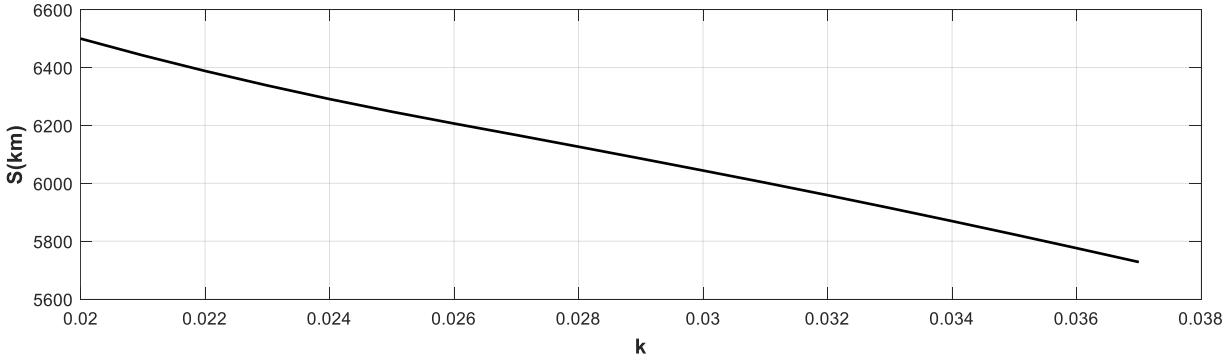


Figure 21 - Variation of Cruise Range with Induced Drag Factor

Figure 21 shows the variation of cruise range with the induced drag factor. Under the same weight and altitude conditions, the lift coefficient remains unchanged, while the corresponding drag coefficient increases with increasing induced drag factor, thereby reducing the cruise range.

3.5 Landing Phase

When calculating the landing field length, the landing distance must be multiplied by a field length factor f_L in accordance with FAR-121.195. For turbine-powered aircraft, the field length factor for a dry runway is $f_L = 1/0.6$, while for a wet runway it is $f_L = 1/0.6 \times 1.15$. Therefore, when calculating the landing field length, it is necessary to consider whether the longest landing distance, namely the landing field length on a wet runway, satisfies the landing field length requirement.

The aircraft has a maximum landing weight of 67,800 kg and is in the approach and landing configuration. The rolling friction coefficient is 0.0075, the braking friction coefficient is 0.5, and the approach speed is $1.3V_s$.

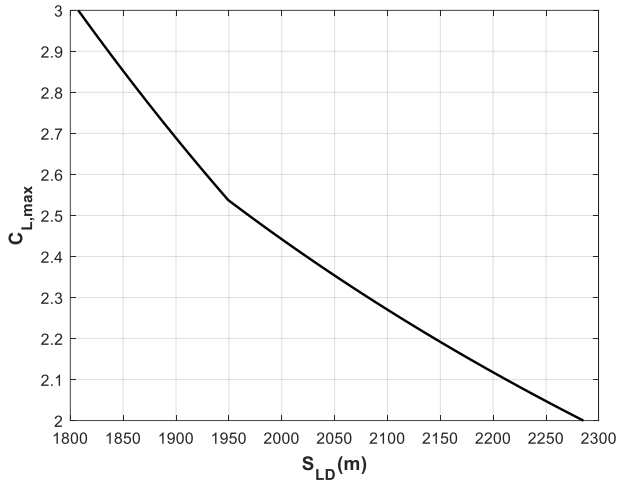


Figure 22 - Maximum Lift Coefficient

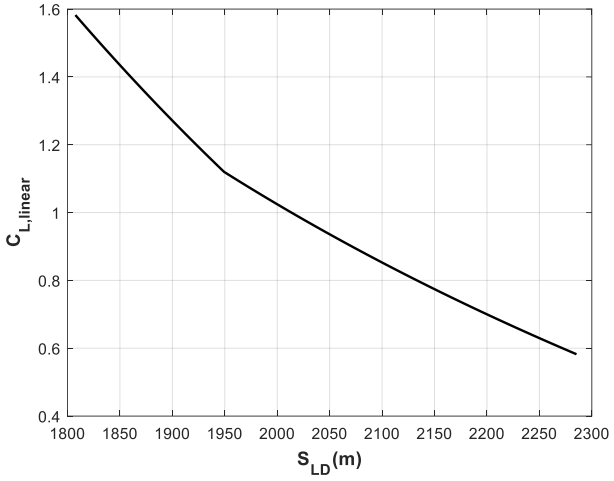


Figure 23 - Linear-Region Lift Coefficient

Based on the aerodynamic requirement analysis, it can be seen that the shorter the landing field length, the higher the requirements for the maximum lift coefficient and the linear-region lift coefficient in the landing configuration. This is because increasing the maximum lift coefficient reduces the aircraft stall speed V_S, which in turn reduces the corresponding approach speed $1.3V_S$, thereby shortening the landing ground-roll distance and reducing the required landing field length.

Under these aerodynamic performance conditions, the actual landing distance of the aircraft is calculated.

Taking the maximum lift coefficient in the landing configuration of 2.72 as an example, the horizontal flight distance in the airborne phase is 357.9 m. The ground distance in the transition phase is 134.7 m.

The numerical simulation results of the ground-roll distance, ground-roll speed, and normal reaction force during the ground-roll phase are shown in Figure 24.

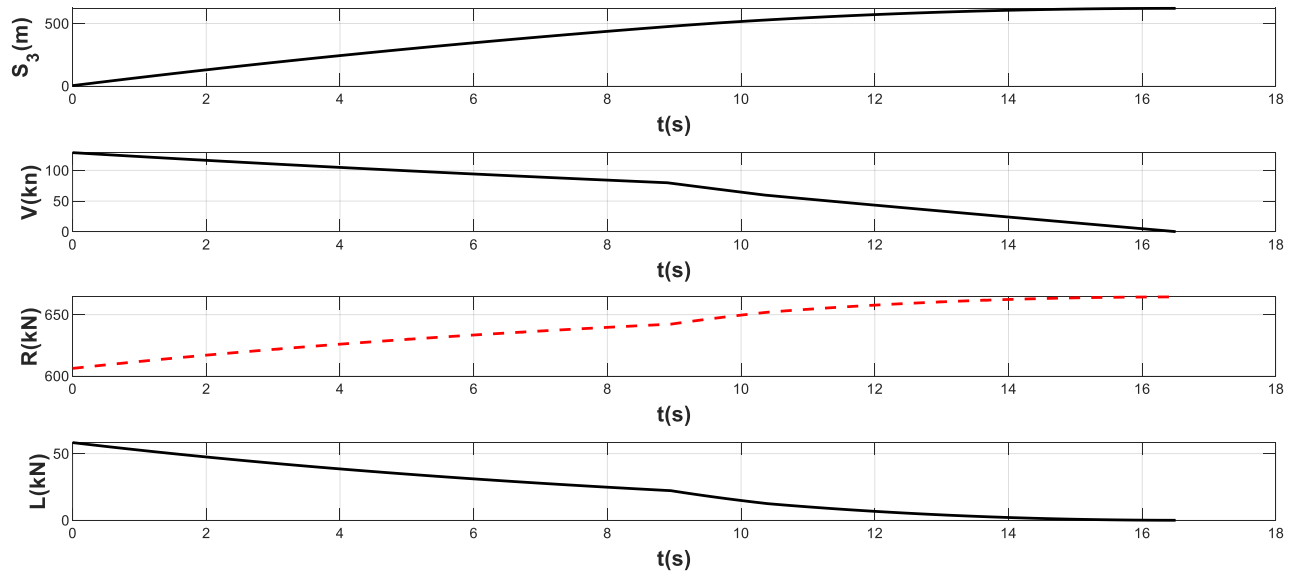


Figure 24 - Simulation of Actual Landing Ground Roll

The ground-roll distance during the ground-roll phase is 591.5 m, and the actual landing distance is 1084 m.

3.6 Function integration design

For ease of use, a software tool was developed in this study to calculate the aerodynamic requirements for each flight phase based on the specified performance metrics. By inputting basic

aircraft parameters, airport parameters, and performance requirements, the aerodynamic requirements can be obtained directly.

All input parameters in the interface are provided with default initial values. If modifications are required, users can simply click the corresponding field and enter the desired values. Figure 25 below shows the input interface.

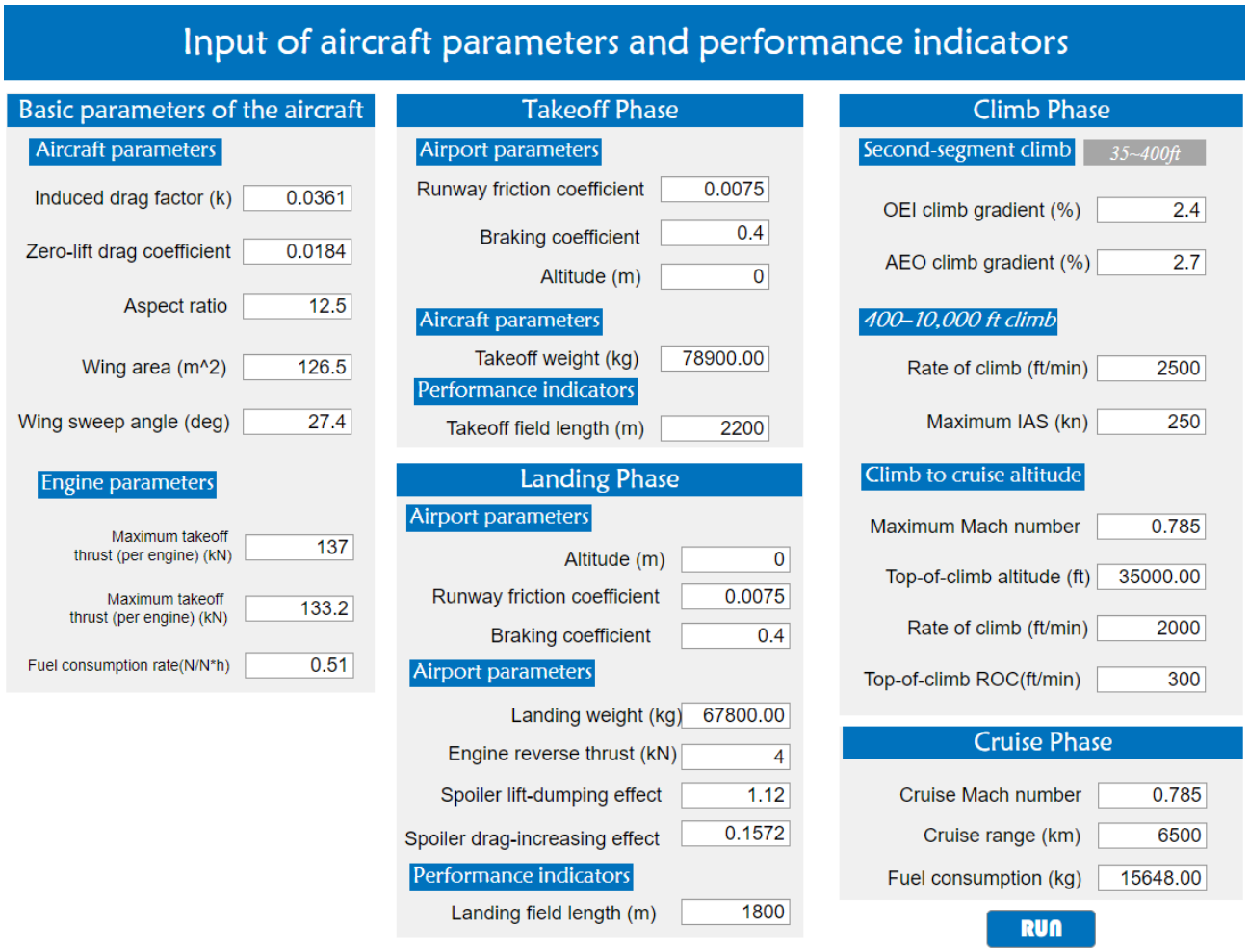


Figure 25 - Aircraft Parameters and Performance Requirements Input Interface

After all required aircraft parameters and performance requirements have been entered, click the "Run" button to start the aerodynamic requirement analysis process. The program will automatically perform the corresponding calculations based on the input data. Depending on the complexity of the analysis and the computational resources available, the calculation may take several seconds to complete. Users are advised to wait until the process finishes and avoid modifying the input data during execution.

Once the computation is completed successfully, the "Aerodynamic Requirement Analysis" interface will automatically appear, displaying the calculated aerodynamic requirements and performance constraints for the selected flight condition. The aerodynamic requirements corresponding to different flight phases can be viewed through the drop-down menu located in the upper-left corner of the interface. Available flight phases include takeoff, second-segment climb, climb to cruise altitude, cruise, and landing as shown in Figure 26 - Figure 29. By selecting a specific flight phase, users can examine the associated aerodynamic performance requirements, including lift coefficient demand, drag characteristics, lift-to-drag ratio requirements, and other relevant design constraints. This feature enables a comprehensive evaluation of aircraft aerodynamic performance throughout the entire flight mission profile.

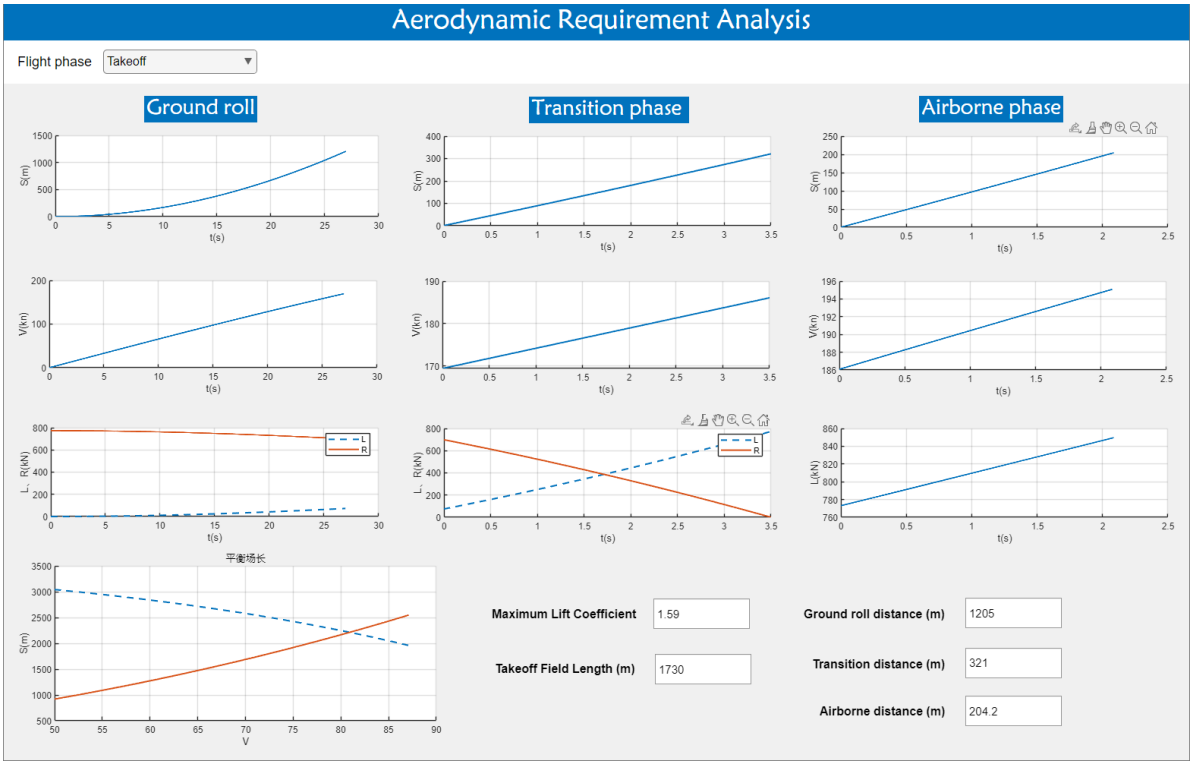


Figure 26 - Takeoff Aerodynamic Requirements

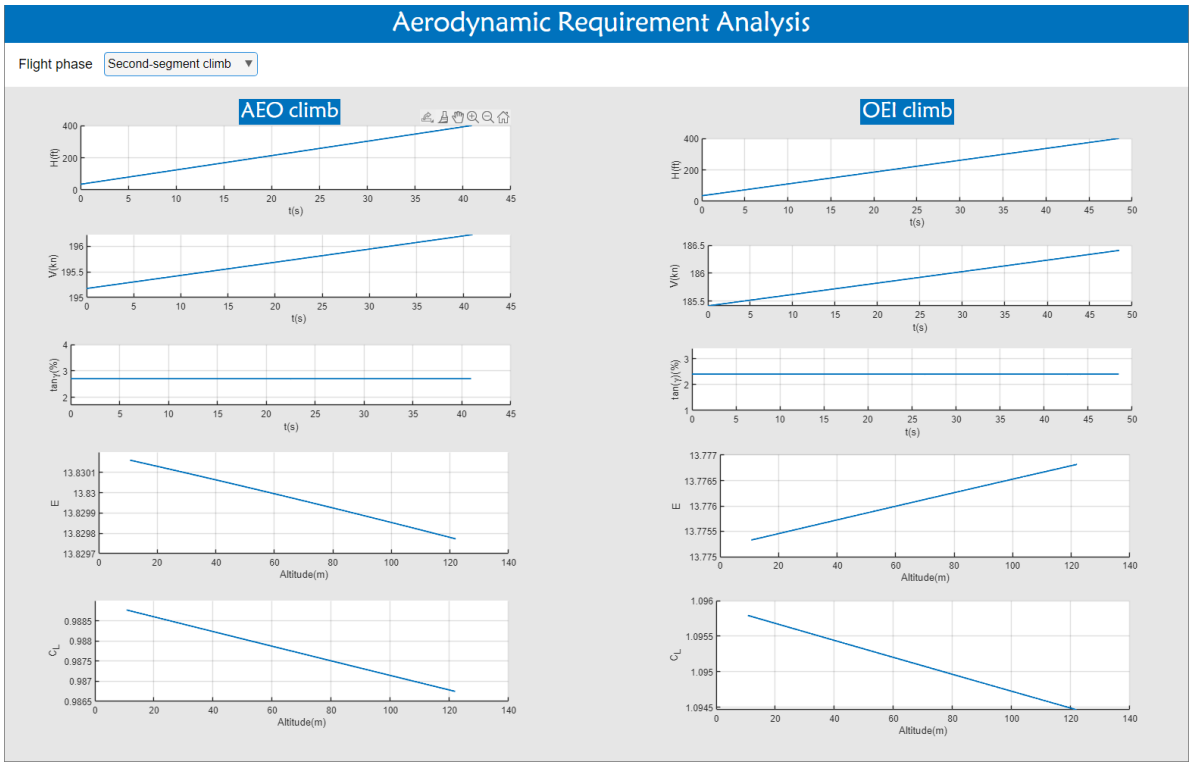


Figure 27 - Second-Segment Climb Aerodynamic Requirements

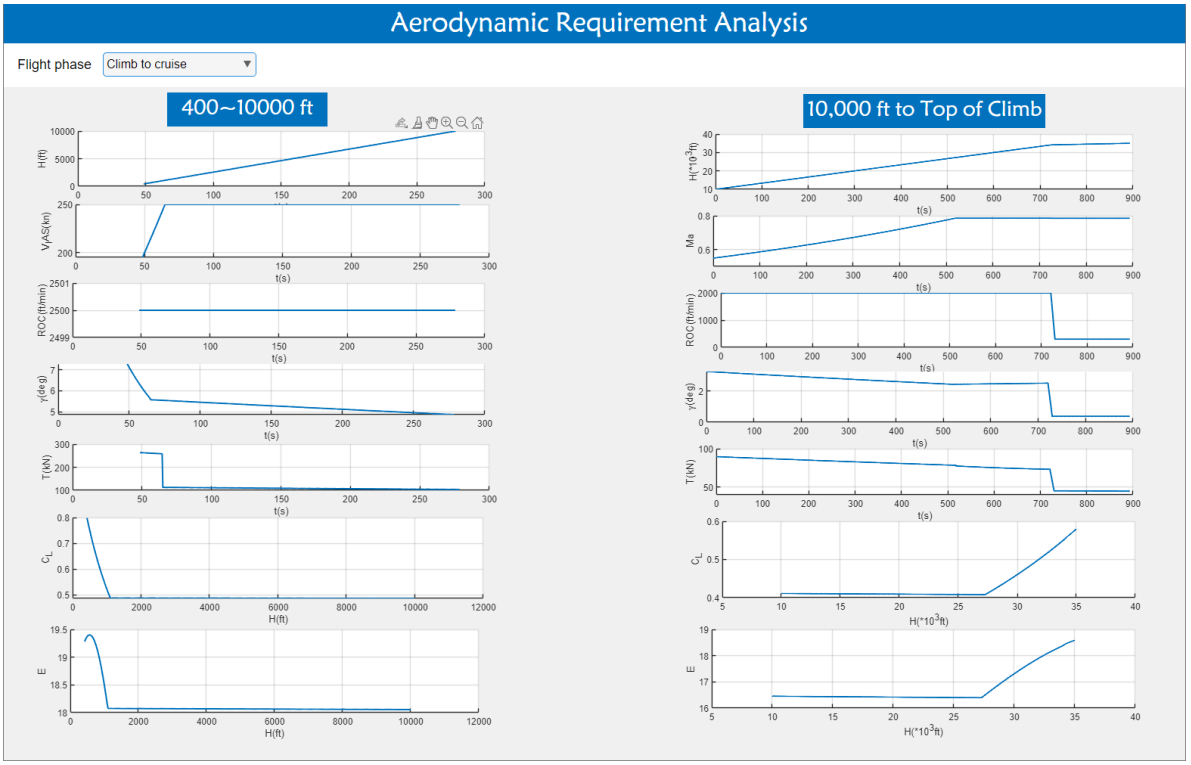


Figure 28 - Climb-to-Cruise Altitude Aerodynamic Requirements

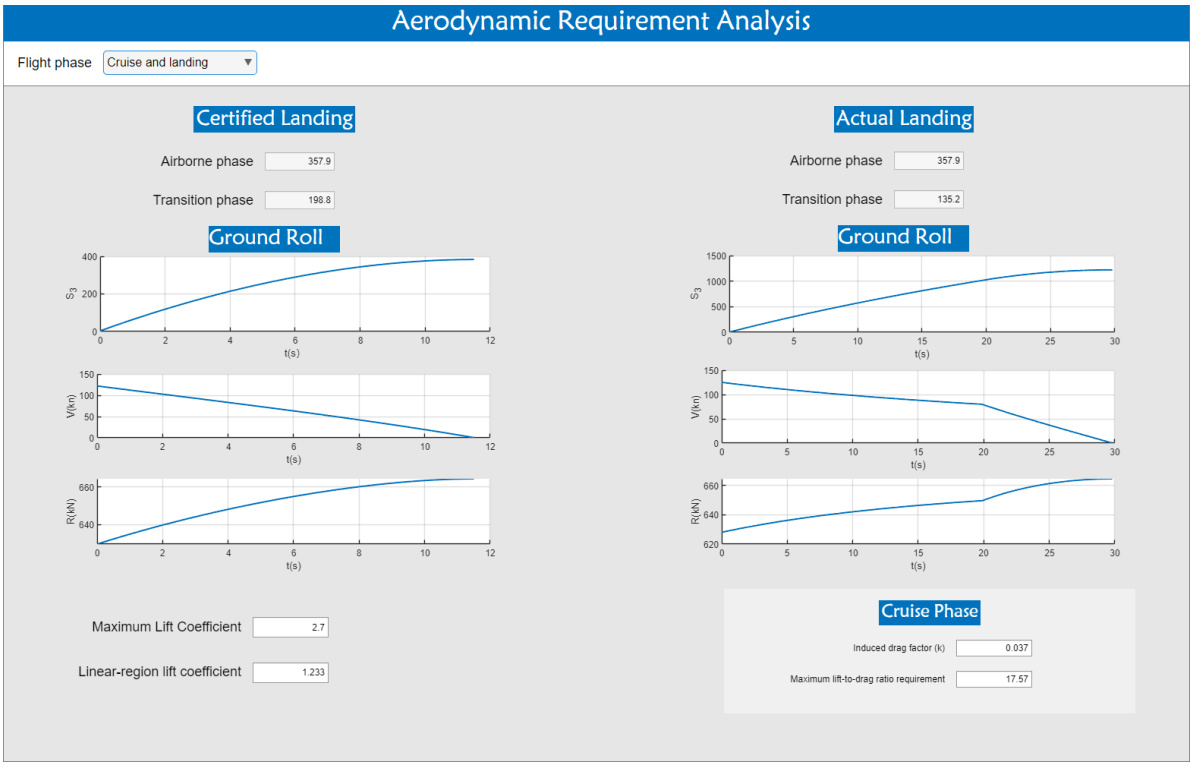


Figure 29 - Cruise and landing Aerodynamic Requirements

4. Conclusion

This paper addresses the issue that aerodynamic parameters are difficult to determine during the modification design of large-aspect-ratio civil aircraft. By prescribing flight performance requirements and integrating airworthiness performance criteria with flight performance indices, the aerodynamic parameter requirements in different flight phases are analyzed. The proposed method provides a reliable and systematic reference for aerodynamic requirements in the preliminary aerodynamic

configuration design of aircraft, effectively avoiding the frequent and time-consuming iterative optimization processes in traditional design approaches. As a result, the preliminary aerodynamic design cycle is significantly shortened, and both design efficiency and directional accuracy are improved.

5. Contact Author Email Address

If you have any question, please mail to: wrq2024200076@mail.nwpu.edu.cn

6. Copyright Statement

The authors confirm that they, and/or their company or organization, hold copyright on all of the original material included in this paper. The authors also confirm that they have obtained permission, from the copyright holder of any third party material included in this paper, to publish it as part of their paper. The authors confirm that they give permission, or have obtained permission from the copyright holder of this paper, for the publication and distribution of this paper as part of the ICAS proceedings or as individual off-prints from the proceedings.

References

[1] 李梁昆.基于起飞性能的高原机场飞机滑跑距离计算研究[D].中国民用航空飞行学院,2024.DOI:10.27722/d.cnki.gzgmh.2024.000082.(In Chinese)

[2] “Aircraft Design: A Conceptual Approach,” Aircraft Design: A Conceptual Approach, Seventh Edition, Jun. 2024.

[3] A. H. Fraser - Mitchell. Fundamentals of Aerodynamics - Fifth edition[J]. Aeronautical journal,2012,116(Feb. TN. 1176):222-223.

[4] “Performance, Stability, Dynamics, and Control of Airplanes, Second Edition,” Jun. 2004.

[5] J. BELDERRAIN and P. PAGLIONE, “Optimal performance of airplanes flying through windshear,” Guidance, Navigation and Control Conference, Feb. 2013.

[6] P. J. Boschetti, P. Gonzalez, and E. M. Cardenas, “Program to Calculate the Performance of Airplanes Driven by a Fixed-Pitch Propeller,” AIAA Atmospheric Flight Mechanics Conference, Jan. 2015.

[7] J. BELDERRAIN and P. PAGLIONE, “Optimal performance of airplanes flying through windshear,” Guidance, Navigation and Control Conference, Feb. 2013.

[8] K. Elferink and H. Visser, “Optimal and near-optimal take-off maneuvers in the presence of windshear,” 2000 World Aviation Conference, Feb. 2013.